MODELLING OF ADIABATIC STEAM STRIPPING OF PAH-WATER BINARY MIXTURE IN MEAN FIELD APPOROXIMATION

A. Jakovics, V. Frishfelds

Faculty of Physics and Mathematics, University of Latvia,
Zellu iela 8, LV-1002 Riga, LATVIA
e-mail: ajakov@latnet.lv

B. Niemeyer, J. Hoehne

GKSS-Forschungszentrum GmbH,
Max-Planck-Straße, 21502 Geesthacht, GERMANY
e-mail: niemeyer@gkss.de

The process of steam stripping of two-component sludge is described in isobaric approximation. The stripping process is split in two stages. The first stage is the diffusion controlled saturation of the partial pressures which goes relatively fast. Next stage is heat transfer controlled evaporation. First, the phase diagram of PAH-water is constructed using solubility data and linear dependence of partial pressures on molar fraction outside miscibility gap. Next, the microscopic model for the estimation of the properties of PAH-water system is discussed in order to improve the empirical approach. Naphthalene-water system is taken as a particular example. Partial pressures and phase diagram are obtained within the model by use of mean field approximation in lattice-gas model, where the size of one type of molecule is considerably larger than that of another.

1. INTRODUCTION

Soils contaminated with PAH (polycyclic aromatic hydrocarbons) are extremely hazardous to living organisms. GKSS research centre has developed and built up a pilot equipment to clean soil polluted with PAH by steam stripping [1]. The average size of previously refined soil particles in experiments lies between 10 and 100 μm. Before treatment, the contaminated soil is mixed up with water to form sludge. This mixture is pushed into the reactor tube through a nozzle using a stream of hot water vapour (see Fig. 1). The PAH are transferred from the sludge to the gaseous steam phase during the steam stripping process. The length of a nozzle is chosen so that the boiling of water does not occur in it, while the temperature reaches nearly 100 °C (see Fig. 2). Strong turbulent conditions are present at the outlet of the nozzle. Thus, overheated steam is efficiently mixed up with the droplets of sludge. Therefore, we can consider a small sub-system (cell) of the resulting mixture that consists of one droplet and vapour around it. The mass ratio of the droplet and vapour equals to their supply ≈1/10. This ratio and initial steam temperature (up to 400 °C) is enough for evaporating all of water in sludge. Steam stripping in the cell can be assumed as nearly adiabatic as the heat exchange between the cell and reactor walls is neglectable in such a short interval of time needed for the process.

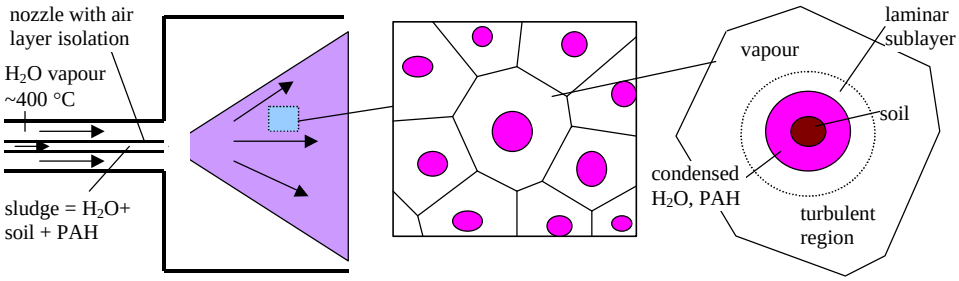

Fig. 1. Spraying of the sludge by superheated steam and steam stripping of PAH contaminated droplets

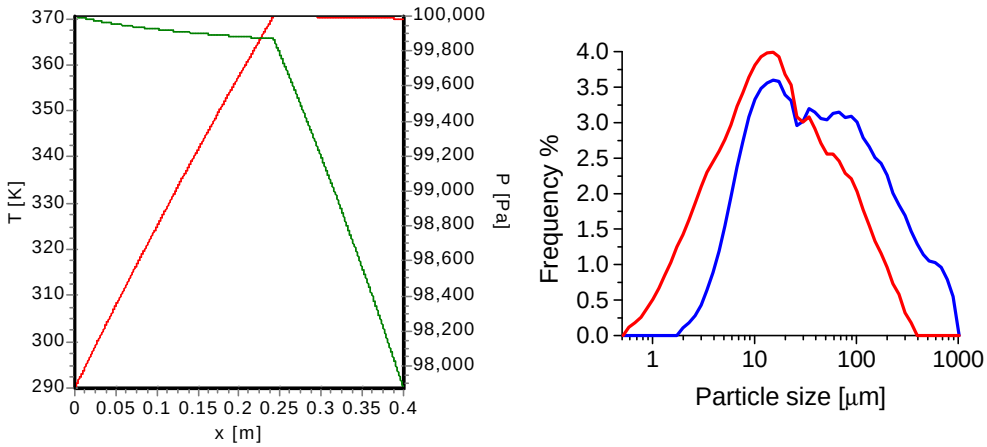

Fig. 2. Increase of temperature and decrease of pressure in a long Cu pipe with a layer of air insulation. The size of pipe in the equipment is about 10 cm, ensuring that boiling of water does not start inside the pipe

Fig. 3. Characteristic distribution of soil particles on their sizes before and after the treatment

The size of soil particles decreases during the treatment in the reactor as shown in Fig. 3. It occurs due to removal of film containing oil and PAH that consolidates several micro particles. The disintegration of soil [1] is neglected and we will discuss only the initial phase of process neglecting desorption. Desorption occurs in the rest part of reactor and is described, e.g., in [2].

2. EMPIRICAL CONSTRUCTION OF PAH-WATER PHASE DIAGRAM

The liquid part of the sludge and vapour consists of two components: water and PAH. One characteristic feature of such a PAH-water system is an extremely small solubility of one component into another. Thus, there exists a wide miscibility gap [3]. The pressure of such system is independent of the PAH fraction inside the miscibility gap. This is shown in *P-x* plane of Fig. 2 by a plateau. The pressure should be approximately proportional to its molar fraction up to the solubility limit. The assumed proportionality means that the activity coefficient does not depend on the molar fraction in this range. Thus, the activity coefficient is the reciprocal of molar solubility [4]. The improvement of the empirical approach will be considered in the last two sections using a microscopic model. At the opposite side of phase diagram the partial pressure increases slightly, - it must tend to Raoult's law at the end. However, both solubilities are so small that there is

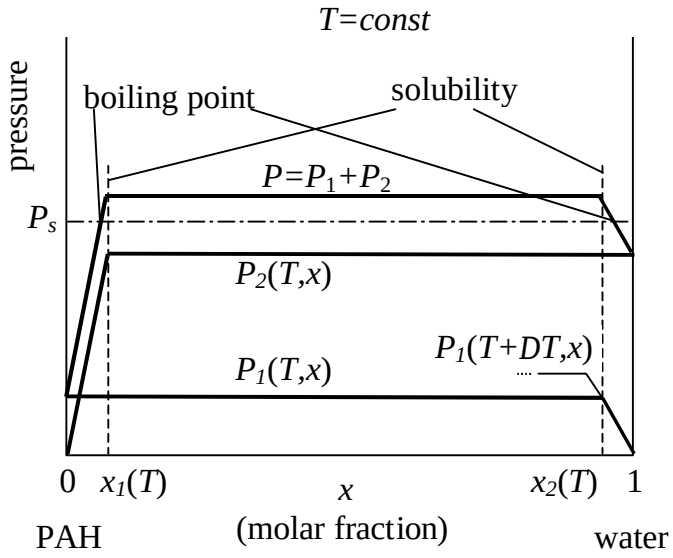

Fig. 4. Partial pressures of the components

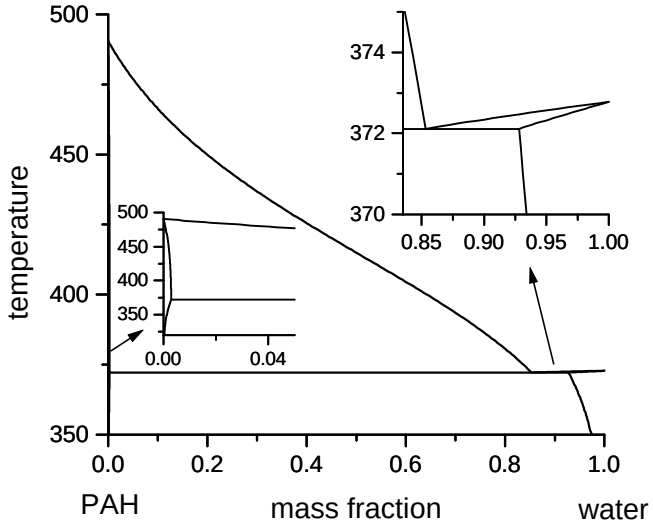

Fig. 5. Constructed phase diagram of naphthalene-water

really no influence of this increase. The total pressure of the system is given by the sum of partial pressures, because water and PAH are relatively inert with respect to each other. Molar solubility follows approximately from Henry's law:

$$S(T) = k \quad (T)P(T), \tag{1}$$

where $P(T)$ is pressure of the component. Let us consider that Henry's constant k_H is nearly independent of temperature. That is of course a rough approximation, as the experimental data show the increase of k_H for PAH in water by an order of magnitude from 298 K to 373 K [5]. The consequence of Henry's law is that the slope of the partial pressure outside miscibility gap (see Fig. 4) does not change with temperature. Thus, we should know the

solubility only at one temperature say at azeotrope T_e. The temperature of the azeotrope T_e, which for the PAH-water system is very close to the boiling temperature of water, can be determined from Dalton's law

$$P_1(T_e) + P_2(T_e) = P_s \tag{2}$$

where P_s is the pressure of the system, $P_1(T)$, $P_2(T)$ are the partial pressures of PAH and water at plateau, respectively. In our case, the partial pressure at plateau equals to pressure of pure component at the same temperature. The data for Antoine approximation of pressure

$$\ln P(T) = A - \frac{B}{T + C} \tag{3}$$

are readily available with some constants A, B, C. An approximation of liquid-vapour data by more complicated formulas, e.g. [6], is useful in broader range of temperatures, but they are worse in particular range of temperatures of steam stripping. Solubilities $x_1(T)$, $1\text{-}x_2(T)$ follow from (1):

$$x_1(T) = x_1(T_e)\frac{P_2(T)}{P_2(T_e)}, 1 - x_2(T) = (1 - x_2(T_e))\frac{P_1(T)}{P_1(T_e)}. \tag{4}$$

The boiling points corresponds to the points where the pressure of the system P_s crosses the sum P in Fig. 2

$$x_{b1}(T) = x_1(T)\frac{P_s - P_1(T)}{P_2(T)}, 1 - x_{b2}(T) = (1 - x_2(T))\frac{P_s - P_2(T)}{P_1(T)}. \tag{5}$$

Applying the Dalton's law again, dew-points are

$$x_{d1}(T) = \frac{P_2(T)}{P_s}, 1 - x_{d2}(T) = \frac{P_1(T)}{P_s}. \tag{6}$$

This equation gives also molar fraction of azeotropic mixture x_e at $T = T_e$. The constructed phase diagram of naphthalene-water by the formulas above is shown in Fig. 5 at various scales.

3. DYNAMICS OF ISOBARIC STEAM STRIPPING

The shape for the droplet should be nearly spherical with soil particle placed at the centre. The coefficient of heat conductivity in condensed material usually is higher than in gases. Therefore, the temperature difference inside the small droplet with diameter ≈100 μm, of course, is ever smaller than in the steam phase while the diameter of the cell is about 3 mm. That could be said also about the concentration of PAH, if the PAH phase is present on the surface of the droplet. The evaporation process predominantly should be heat transfer controlled as $q >> \frac{i}{2}kT$ with q - heat of evaporation per one molecule, $i = 5 \div 6$ - degrees of freedom, k – Boltzmann constant. Therefore the distribution of PAH and water in vapour phase is almost homogeneous.

Let us separate the process in two stages. The saturation of partial component pressures in vapour phase and sludge appears in the first stage of the process which takes place in very small interval of time compared to the second stage of the process. Therefore, the absolute values of diffusion coefficients are less important. At the second stage the binary mixture is evaporating due to heat transfer towards droplet. This process is heat transfer controlled and follows boiling and dew curves in the phase diagram.

3.1. SATURATION OF PARTIAL PRESSURES

The average velocity of molecules in gas is inversely proportional to the square root of their molar mass. On other hand, the mean free path is inversely proportional to the square of the size of molecule. Hence, the ratio of diffusion coefficients of PAH and water in steam is

$$\frac{D_1}{D_2} \approx \sqrt{\frac{m_2}{m_1}} \left(\frac{r_1 m_2}{r_2 m_1} \right)^{2/3}, \tag{7}$$

where m is molar mass, r - density in condensed phase, indexes: 1 - PAH, 2 - water. Steam initially contains no PAH. Hence, PAH transfers from sludge to vapour. At the same time, the water pressure in the vapour phase is higher than that of the droplet as the initial temperature is kept lower than the temperature of azeotrope. The molar amount of components M_1, M_2 changes according to

$$\frac{\partial M_1}{\partial t} \sim D_1 \left(P\ (1-y) - P_1(T,x) \right), \frac{\partial M_2}{\partial t} \sim D_2 \left(P_s y - P_2(T,x) \right), \tag{8}$$

where x, y are the molar fraction of water in droplet and vapour, respectively. Effects of the surface tension are unimportant for the sizes of the droplet exceeding micrometer scale. Due to condensation of water and evaporation of PAH, some heat is created:

$$\Delta Q_q = q_1(T,x) m_1 \Delta M_1 + q_2(T,x) m_2 \Delta M_2, \tag{9}$$

where $q_1(T,x)$, $q_2(T,x)$ are heat of evaporation per one mole of the respective component. This heat, furthermore, changes the temperature of the droplet:

$$\Delta Q_c = (C_{p1}(T) M_1 + C_{p2}(T) M_2 + c_s m_s) \Delta T, \tag{10}$$

where $C_{p1}(T)$, $C_{p2}(T)$ are molar heat capacities of components; c_s, m_s are heat capacity and mass of soil particle inside the droplet. The heat of evaporation is related to saturation pressure by Clausius-Clapeyron law:

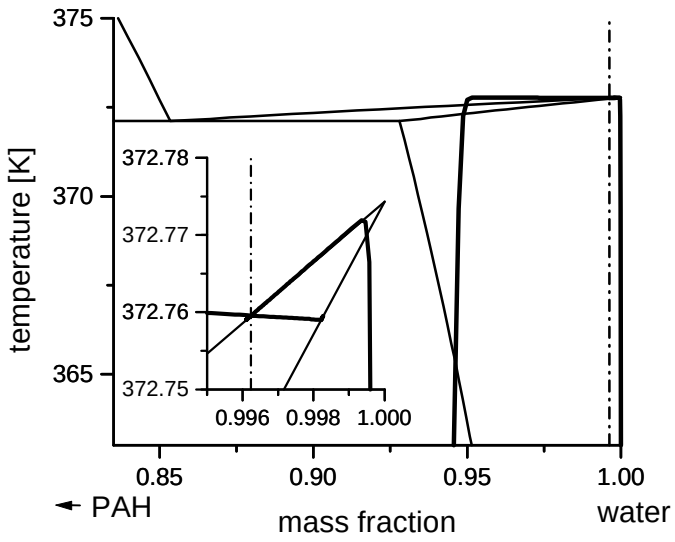

Fig. 6. Dynamics of the stripping in phase diagram, Fig. 5. Thick curves correspond to droplet and vapour at surface temperature. Dot-dashed line – total mass fraction x_t in cell

$$q(T) = \frac{\partial P}{\partial T} T \left(\frac{1}{r_g(T)} - \frac{1}{r_l} \right), \tag{11}$$

where r_g, r_l are densities in gas and liquid phase, respectively. The constructions in Fig. 2 show that heats of evaporation are

$$q_1(T,x) = \begin{cases} q_1(T), & x \le x_2(T) \\ 0, & x > x_2(T) \end{cases}, q_2(T,x) = \begin{cases} q_2(T), & x \ge x_1(T) \\ 0, & x < x_1(T) \end{cases}, \tag{12}$$

where $q_1(T)$, $q_2(T)$ are heat of evaporation of pure components. The characteristic scenario of diffusion is shown in Fig. 6. One can split the process again in two subparts due to much slower diffusion of PAH (7) in the steam, i.e., water pressure saturates first, and PAH evaporates afterwards relatively slowly. As can be seen, the droplet curve ends at boiling point and vapour line at dew point. That acts as the initial condition for the second stage of the process described below. This position lies on the same side of phase diagram with respect to azeotropic mixture x_e as the fraction of water in all PAH-water cell x_t does. The position of x_t is shown by dot-dashed line in Fig. 6. For example, diffusion ends at the right side of the azeotrope for naphthalene in Fig. 6 but for pyrene in Fig. 7. – at the opposite side.

Due to initial condensation of water the size of droplet first increases as shown in Fig. 8. The further decrease of the droplets size is caused by evaporation described below.

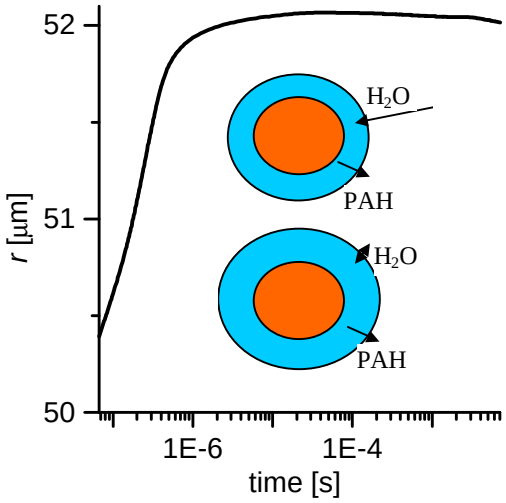

Fig. 8. Initial growth of the particle

3.2. HEAT TRANSFER CONTROLLED EVAPORATION

The second stage of the process takes place so that the water fraction in droplet coincides with boiling curve, while water fraction in vapour - with dew curve. It can be easily simulated by equalisation of the right hand side of (8) with zero. The evaporation finishes at point, where dew curve crosses the total fraction x_t, when all the mixture is evaporated. That can be seen in enlarged scale of Fig. 6 by small increase of temperature after the end of the first stage.

If the steam fraction and its temperature is insufficient, the process stops at the equal temperature of steam and droplet. The radiation heat transfer is unimportant for characteristic temperatures in reactor and sizes of droplets below millimetre. The use of

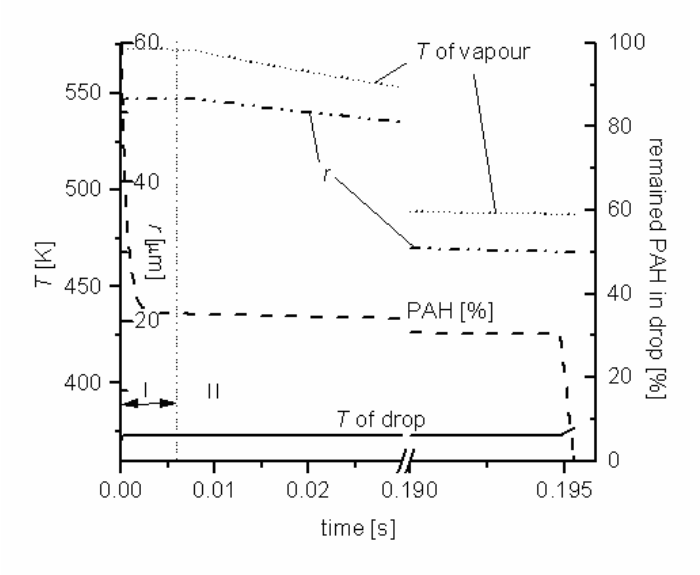

Fig. 4. Behaviour of the temperature of droplet and vapour, radius of droplet, and amount of PAH remained in the drop at steam stripping of pyrene. I – diffusion controlled approach, II – heat transfer controlled approach

Stokes law show that initial average velocity difference between steam and vapour decreases faster than evaporation of sludge. However, there exists some local stochastic difference of velocities and the heat and mass transfer between vapour and droplet is turbulent that increases heat transfer to the droplet. The coefficient of heat transfer is approximately proportional to the temperature difference of droplet and steam. The proportionality coefficient can be interpreted by some effective thickness of relatively thin laminar sublayer around the droplet. The temperature and concentration in the remaining turbulent region is almost constant. Heat transfer from steam to droplet

$$\frac{\partial Q_l}{\partial t} = \frac{4p}{\frac{1}{r} - \frac{1}{r + d_{lam}}} \int_T^{\gamma} l(T)dT \tag{13}$$

must be added in (10), where r is the radius of the droplet, d_{lam} – thickness of laminar sublayer, $l(T)$ – coefficient of heat conductivity in steam, T_v – temperature of vapour in turbulent region. This heat transfer causes the cooling of vapour

$$\Delta Q_l = -\left(\frac{i_1 + 2}{2} M_{1v} + \frac{i_2 + 2}{2} M_{2v}\right) R \Delta T_v, \tag{14}$$

where R is universal gas constant; i_1, i_2 – degrees of freedom; M_{1v}, M_{2v} – molar amount of components in vapour phase.

The degree of PAH cleaning, temperatures and radius of the droplet during steam stripping of pyrene-water system are shown on Fig. 7. The time scale of diffusion controlled approach here is chosen arbitrarily. The size of the droplet increases in first stage of the process but decreases more rapidly in next stage reaching the size of the soil particle. As the total fraction of water is lower than of azeotrope, the water fraction in droplet decreases up to the moment when the solubility limit of water in pyrene is reached. Afterwards, strong evaporation of pyrene and increase of the temperature of the droplet takes place.

The total size of the cell in Fig. 1 decreases by approximately 3 % in the described isobaric evaporation. However, the pressure would remain constant only if the scattering angle in Fig. 1 is close to zero. In general, the pressure of the system decreases behind the opening of the pipe as the vapour-sludge mixture diffracts. The temperature would remain approximately constant for laminar diffraction of ideal gas. Thus, the non-monotonous decreases of remained PAH content in droplet is possible. However, that cumbers the understanding of the process while the qualitative behaviour of the process does not change.

4. MICROSCOPIC MODEL OF LATTICE

Let us improve now the empirical model for PAH-water system with its wide miscibility gap. The wide miscibility gap occurs because of weak interaction between PAH and water molecules in comparison with the interaction between PAH-PAH and water-water molecules. These interactions can be easily included into lattice-gas model, in such a way that water and PAH molecules can situate only at certain sites of the “imaginary” lattice (positions in the lattice). The interactions occur between molecules situated at neighbouring sites. The size of the organic PAH molecule is much larger than that of water. This can be considered assuming that PAH molecule occupies several sites while water molecule occupies only one. Example of two-dimensional simulation of such a system at two different temperatures is shown in Fig. 9.

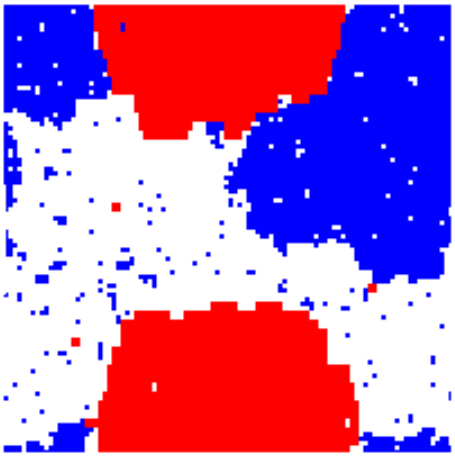

Fig. 9. Monte-Carlo simulations of PAH-water system near equilibrium at T=300 K. Larger molecules: PAH, smaller: water. Periodic boundary conditions

As can be seen from Fig.9, PAH fraction condenses at higher temperature as the boiling temperature of PAH is higher than that of water. However, the boiling temperature of the mixture depends on the fraction of both components in the system. The analysis of phase transitions will be made using mean field approximation [7]. It neglects the correlations in the system.

5. STATIONARY CASE

It is impossible to find analytically the accurate expression of entropy if the size of one molecule is larger than another. In order to simplify the analysis, it is assumed that

larger molecules can occupy only fixed positions in the lattice which guarantees that each PAH molecule do not edge into another. These positions are chosen in a way that there is absence of free sites in the pure PAH system. Free energy F^l of such a liquid phase in the mean field approximation [8] neglecting the presence of vacancies is

$$F^l = -\frac{1}{2N}\left[l_{11}aN_1^2 + l_{12}(a+1)N_1N_2 + l_{22}N_2^2\right] + kT\left[N_1 \ln\frac{aN_1}{N} + \frac{N_2}{a}\ln\frac{N_2}{N}\right], \quad (15)$$

where $N \equiv aN_1 + N_2$ is the number of sites in the system, N_1, N_2 are numbers of PAH and water molecules, respectively; l_{11}, l_{12}, l_{22} are binding energies between PAH-PAH, PAH-water and water-water, respectively; a is the ratio of volumes between molecule of PAH and water. The values of the molar masses and densities of pure components show that the volume ratio a is 6.77 for naphthalene, while a = 8.83 for pyrene. The lattice-gas model has to be used also for gaseous phase. The free energy here is

$$F^g = kT\left[N_1^g \ln\frac{N_1^g}{N^g} + \frac{1-a}{a}(N^g - aN_1^g)\ln\frac{N^g - aN_1^g}{N^g} + N_2^g \ln\frac{N_2^g}{N^g} + (N^g - aN_1^g - N_2^g)\ln\frac{N^g - aN_1^g - N_2^g}{N}\right], \quad (16)$$

where N^g is the number of sites in gaseous phase; N_1^g, N_2^g are numbers of PAH and water molecules in gas phase, respectively. The interaction in gaseous phase has been neglected as the concentrations here are very small $aN_1^g + N_2^g << N^g$. In equilibrium case, the chemical potentials m_1, m_2 of components in both phases are equal:

$$\frac{\partial F^l}{\partial N_1} = \frac{\partial F^g}{\partial N_1^g} = m_1, \frac{\partial F^l}{\partial N_2} = \frac{\partial F^g}{\partial N_2^g} = m_2. \quad (17)$$

The partial pressure for ideal gas is proportional to the density of respective component. This assumption allows to obtain equilibrium pressures at phase boundary:

$$P_1(T,C) = P_{1eq}(T)(1-C)\exp\left[\frac{sC^2}{2kT}\right], P_2(T,C) = P_{2eq}(T)C^{1/a}\exp\left[\frac{s(1-C)^2}{2akT}\right], \quad (18)$$

where $s = l_{11} - l_{12}(a+1) + l_{22}a$; $C = \frac{N_2}{N}$ is the volume fraction of water in condensed phase. The parameters l_{11}, l_{22} which depend on temperature are found in such a way that for pure substances one gets corresponding saturation pressures $P_{1eq}(T)$ and $P_{2eq}(T)$ found in literature [6]. The above mentioned approximation of entropy leads to impossibility of separate water molecule to enter in condensed PAH phase. Thus, the Henry's law is fulfilled in this model only for molecules with higher molecular volume - in our case PAH. However, the more accurate Monte-Carlo simulations show that Henry's law is fulfilled if the condensed phase contains vacancies. The partial pressure of PAH vs. water is shown in Fig. 10. Below the temperature of azeotrope T_e, the pressure curve crosses itself and the cross-point corresponds to phase transition. In this case it is solubility limit. The equality of pressures follows from (17) as the chemical transformation does not occur at phase transition. The energetic parameter s is taken as independent of temperature. Its value is estimated from PAH solubility in water at T_e. At higher temperatures, the pressure of the system P=1 bar (dotted line) crosses the sum $P_1(T,C) + P_2(T,C)$ and the cross-points

(hollow circles) are the boiling points of mixture. The molar fraction of water at dew points is the same as ratio between water pressure $P_2(T,C)$ in the hollow cross-point and total pressure P. That is the consequence of Dalton's law.

The graphically obtained phase transition points of Fig. 10 allow to build the phase diagram in Fig. 11. Rather high solubility of water in PAH is caused by the approximation of entropy for molecules with different sizes.

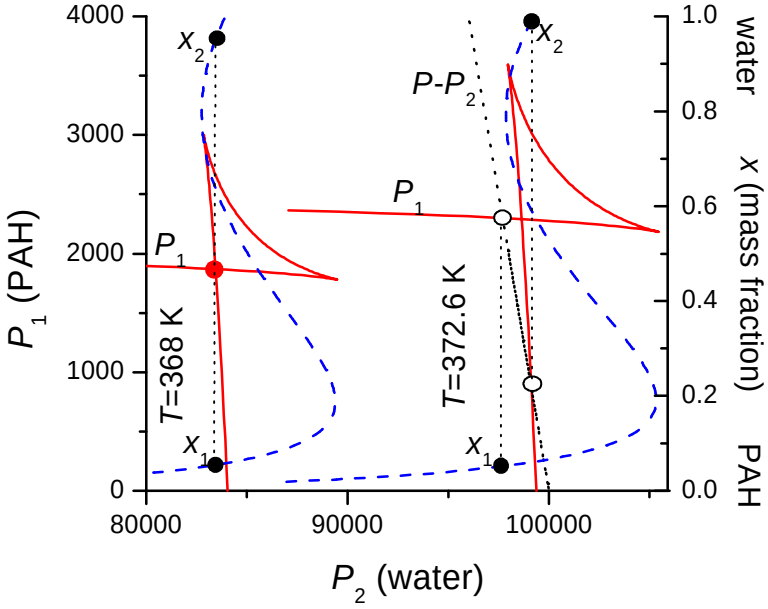

Fig. 10. Partial pressure of naphthalene vs. water (solid curve) at temperatures lower and higher than T_e. Dashed curve – mass fraction of water. x_1, x_2: phase transition points

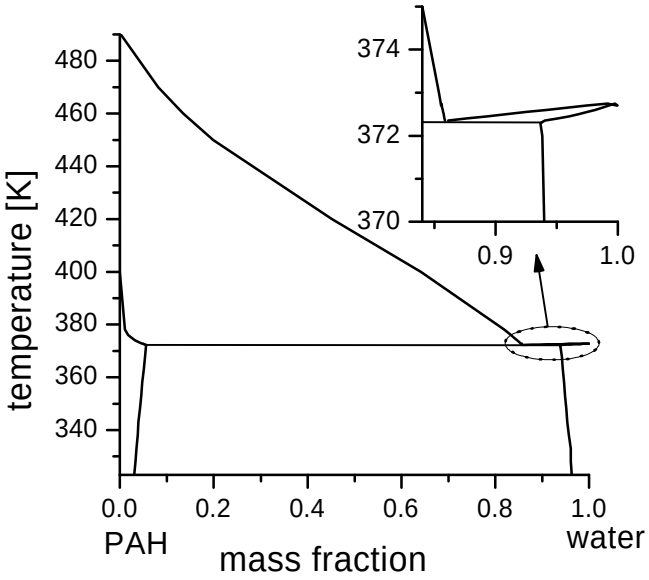

Fig. 11. Constructed phase diagram of naphthalene-water basing on partial pressures in Fig. 10

6. CONCLUSIONS

The mean field approximation of microscopic lattice-gas model allows obtaining the correct behaviour of partial pressures of binary mixture if the saturation pressures of individual components are known. The wide miscibility gap in PAH-water system is caused by comparatively weak interaction between different molecules. More accurate and time consuming Monte-Carlo simulations allow testing of the obtained equations for phase equilibrium.

The saturation of pressures during steam stripping finishes at the same side in phase diagram with respect to azeotropic fraction as total fraction of the system does. The size of the system decreases at isobaric conditions despite of evaporation of the droplet.

REFERENCES

1. Höhne, J, Eschenbach, A., Niemeyer, B.: Minimization of waste by sludge treatment applying the steam stripping process. Proceedings of International Symposium on Waste Management in Asian Cities, Hong Kong, October 23-26, 2000.
2. Wietstock, P., Wilichowski, M., Niemeyer, B.: Entfernung von PAK aus feinkörnigen Böden durch Niedertemperatur-Desorption. Chem.-Ing.-Tech., Vol. 70, 1998, pp. 1167.
3. Kirschbaum, E.: *Destilier un Rektifiziertechnik*. Springer-Verlag, Berlin, 1969.
4. Hwang Y.-L., Olson, J.D., Keller, G.E: *Steam stripping for removal of organic pollutants from water. 2. Vapor-liquid equilibrium data*. Ind. Eng. Chem. Res. Vol. 31, 1992, pp. 1759-1768.
5. Ten Hulscher, Th.E.M., van der Velde, L.E., Bruggeman, W.A.: Temperature dependence of Henry's law constants for selected chlorobenzenes, polychlorinated biphenyls and polycyclic aromatic hydrocarbons. Environmental Toxicology and Chemistry, Vol. 11, 1992, pp. 1595-1603.
6. Yaws, C. L.: *Chemical properties handbook*. McGraw-Hill, New York, 1999.
7. Balescu, R.: *Equilibrium and nonequilibrium statistical mechanics*. Vol. 1. John Wiley and Sons, New York, 1977, p. 405.
8. Ziman, J. M.: *Models of disorder*. Cambridge University Press, Cambridge/London, 1979, p. 580.

PAO-udens binaras sistemas adiabatiskas “izgerbšanas” ar tvaiku modelesana videja lauka tuvinajuma

A. Jakovics, V. Frishfelds, B. Niemeyer, J. Hoehne

Divkomponenšu maisijuma “izgerbšanas” process ar udens tvaiku ir aprakstits izobariska aproksimacija. „Izgerbšanas“ process tiek sadalits divas stadijas. Pirmaja stadija notiek parcialo spiedienu piesatinašanas difuzijas kontroleta procesa, kas ir relativi atrs. Nakamaja stadija notiek siltuma parneses kontroleta iztvaikošana. Sakuma PAO (policikliskie aromatiskie ogludenraži) un udens fazu diagramma ir uzkonstrueta, ja parcialie spiedieni ir lineari attieciba pret molaro frakciju arpus škidamibas diapazona. Lai uzlabotu šo empirisko modeli, tiek apskatits mikroskopiskais modelis PAO-udens sistemas ipašibu petišanai. Ka atsevišks piemers izveleta naftalena-udens binara sistema. Parcialie spiedieni un fazu diagramma šaja modeli tiek ieguti, izmantojot videja lauka tuvinajumu režga gazei, kura viena tipa molekulas izmers ir ieverojami lielaks par otru.